Performance and stability of diaminotoluene-based polyamide composite reverse osmosis membranes incorporated with additives and cast on polyester fabric

Mohamed Said[a,b,*], Shaker Ebrahim[a], Ali Gad[a], Sherif Kandil[a]

[a]*Department of Materials Science, Institute of Graduate Studies and Research, Alexandria University, 163 Horreya Avenue, El-Shatby, P.O. Box 832, Alexandria, Egypt, Tel. +201024604959; Fax: +2035603053; email: mohamedsaid@alexu.edu.eg (M. Said), Tel. +201021309751; Fax: +2034285792; email: shaker.ebrahim@alexu.edu.eg (S. Ebrahim), Tel. +201114454566; email: aligad2003@yahoo.com (A. Gad), Tel. +201003400746; email: s.kandil@usa.net (S. Kandil)*
[b]*Abu Qir Fertilizers and Chemical Industries Co., Postal Code 21911, El-Tabia, Rashid Road, Alexandria, Egypt*

ABSTRACT

This work aims to enhance the performance of polyamide (PA) thin-film composite (TFC) reverse osmosis membranes prepared by the interfacial polymerization of 2,6-diaminotoluene and trimethyl chloride on polysulfone support membrane. The effect of incorporation of triethylamine, isopropyl alcohol and camphor sulfonic acid in the aqueous phase solution on the casted TFC membrane on non-woven polyester was investigated. The prepared membranes were characterized by X-ray diffraction, scanning electron microscopy and contact angle measurements. The results showed that the permeability and desalination stability of the PA membranes were remarkably enhanced. The membrane water flux was increased to 25.3 L/m^2 h in 10 g/L NaCl feed solution at 18 bar, while the salt rejection was 99.46%. For feed aqueous solution containing 35 g/L NaCl, the membrane has exhibited a salt rejection of 98.45% and the water flux has increased to 17.1 L/m^2 h at 35 bar. The desalination stability has remarkably enhanced and the membrane could withstand high operating pressures without permeate more salts. In addition, the energy consumed by PA-TFC membrane was reduced to 1.13 kWh/m^3.

Keywords: Desalination; Membrane performance enhancement; Polyamide; Reverse osmosis; Thin-film composite membranes

1. Introduction

Reverse osmosis (RO) is effectively used for water desalination and industrial water reuse [1]. The interfacial polymerization (IP) method is widely used for the synthesis of thin-film composite (TFC) membranes [2]. The unique advantage of TFC membranes is the possibility to independently optimize both the porous support and the skin layer for their specific function to maximize the overall membrane performance [3,4]. TFC membranes with a polyamide (PA) top active layer are the most popular commercial form of RO and nanofiltration membranes. The PA-TFC membrane consists of a thin dense and selective PA barrier layer laminated on a porous polysulfone (PS) substrate [2,3].

The PA thin layer chemistry, which is an inherent property of the monomers employed in IP reaction, and the preparation conditions are the two important factors that determines the performance of the PA-TFC membranes [5].

Generally, the TFC membranes fabricated from aromatic PA have low water permeability due to the excessive tight cross-linking and low free volume of the PA active layers. Many approaches have been utilized to make PA-TFC membranes with better water flux [6–9]. The additives incorporation in the aqueous phase has been used to improve the water flux of the PA-TFC membrane without a significant loss in its salt rejection. The presence of additives in aqueous or organic phase solution is an important parameter in altering the structure of PA layer [2,10,11].

In a previous work, PA-TFC membranes were prepared by the IP reaction of 2,6-diaminotoluene (DAT) and trimethyl chloride (TMC) [12]. The preparation conditions

---

* Corresponding author.

were systematically studied and optimized to include 1 wt% of DAT for 2 min soaking time, 0.15 wt% of TMC for 30 s reaction time and 75°C curing temperature for 5 min to give the highest membranes performance. The prepared PA membranes exhibited a salt rejection of 99.54% with water flux of 11.42 L/m^2 h in 10 g/L NaCl feed solution and at 18 bar operating pressure. In addition, for a feed solution of 35 g/L NaCl the membranes exhibited a salt rejection of 98.25% and water flux of 9.3 L/m^2 h at 35 bar. The water flux and performance stability of the resulting membranes were found to be relatively low and need further improvements to be suitable for commercial applications. The aim of the current work is to enhance both water flux and performance stability of the PA-TFC membranes for water desalination while maintaining the salt rejection. The performance stability means to enhance the membrane capability to withstand high operating pressure without compaction or deformation. The effect of incorporating triethylamine (TEA), isopropyl alcohol (IPA) and camphor sulfonic acid (CSA) additives in the DAT aqueous solution on the membranes performance was investigated. Also, the effect of casting the PA membrane on non-woven polyester fabric was studied.

2. Materials and methods

2.1. Materials

PS pellets (molecular weight 60,000 product of Acros Organics, USA) were used as a supporting material for the PA-TFC RO membranes. *N*-Methylpyrrolidone (NMP; Fluka Chemie, Switzerland) was used as a solvent. DAT (99%), *m*-phenylenediamine (MPD; 99%) and TMC (98%) were supplied by Acros Company. *N*-Hexane (95%) was supplied by TEDIA Company, USA. NaCl was supplied by MP Biomedical (France) to prepare the salt feed solution. TEA (liquid, 99.5%; Fisher Company, USA) and IPA (Scharlau Company, Spain) were used as additives in the aqueous phase solution and its pH value was adjusted using CSA (Sigma-Aldrich, USA). The polyester non-woven fabric was supplied by Freudenberg Vliesstoffe Company, Germany.

2.2. Preparation of the polysulfone support membrane

In this work, the PS membranes were prepared using phase inversion technique. The PS membrane preparation procedure was mentioned in our previous work [12].

2.3. Preparation of the PA membranes

The PA-TFC membranes were prepared by the IP technique between DAT and TMC at the optimal polymerization conditions. DAT is easily dissolved in aqueous solution and more stable compared with light sensitive MPD monomer. In addition, DAT can be easily removed from the surface of PS membrane without excess aqueous droplets. The aqueous solution contained 1 wt% of DAT, TEA (1, 2, 3, 4 and 5 wt%), IPA (2, 4, 6, and 8 wt%) and 6 wt% of CSA. The aqueous solution was prepared by adding different concentrations of TEA, IPA and 6 wt% of CSA to deionized water (75–80 mL) under vigorous stirring. After complete dissolution of the mixture, deionized water was added to provide a total solution

volume of 100 mL. Finally, DAT (1 wt%) was added to the 100 mL TEA–IPA–CSA mixed aqueous solution.

2.4. Casting the PA membranes on non-woven polyester fabrics

The PS solution was prepared and casted over a commercial non-woven polyester fabric with a thickness of 150 μm taped to a clean glass plate. The upper polyester surface was wetted previously by NMP and left for 3 h before casting the PS solution. After casting the solution over the non-woven fabric, the glass plate was immersed in deionized water at room temperature. The non-woven fabric with the supported PS films was removed from the water bath after 1 h and was separated from the glass plate. The membranes were subsequently washed and stored in deionized water bath for at least 24 h until the solvent was removed.

2.5. Energy consumption of PA membranes

The energy consumed by the primary feed pump for pressurizing the feed water accounts for the major portion of the total energy consumption for a desalination process (80.6%). The specific energy consumption (SEC) of the primary pump is calculated from the following equation [13]:

$$\text{SEC}_{\text{pump}} = \frac{W_{\text{pump}}}{Q_p} = \frac{Q_{f\,\Delta P}}{Q_p} \tag{1}$$

where W_{pump} is the pump work, Q_f is the feed flow rate (L/min), Q_p is the permeate flow rate (L/min) and ΔP is the transmembrane pressure difference (bar).

2.6. Characterization techniques

2.6.1. X-ray diffraction

X-ray diffraction (XRD) scans were carried out (using X-ray 7000 Shimadzu, Japan) at room temperature in the Bragg angle (2θ) in the range of 10°–80°. The X-ray source was a Cu target with settings of 30 kV and 30 mA, with scan speed of 4°/min. The PA membranes were prepared at 1 wt% of DAT or MPD for 2 min soaking time, 0.15 wt% of TMC for 30 s reaction time, 75°C curing temperature for 5 min, 6 wt% CSA, 3 wt% TEA and 4 wt% IPA.

2.6.2. Scanning electron microscopy

Cross-sectional, surface and bottom images of the PA membranes were obtained using scanning electron microscopy (SEM-XL 30 JEOL). The morphological cross-section images of the PA membranes were snapped under liquid nitrogen to give a generally consistent and clean break. The membranes were sputter coated with a thin film of gold. The membranes were mounted on a brass plate using double-sided adhesion tape in a lateral position. The thicknesses of the TFC membrane layers were calculated from the cross-section of the SEM images using the digimizer software.

2.6.3. Contact angle measurements

The contact angle of the PA membranes surfaces was measured using Rame-Hart Instrument Company, France.

A drop of distilled water (2 μL) was placed on the RO membrane surface (3 cm × 2 cm) using a microsyringe (Hamilton Company, Reno, NV). The contact angle was the average of five measurements at different positions on the surface within 10 s after the water drop was placed on the surface.

2.6.4. Salt rejection and flux measurements of the PA membranes

The PA membranes performance (area 42 cm²) was conducted using a cross-flow RO unit (CF042, Sterling, USA) with a feed flow rate of 1 L/min as was mentioned in our previous work [12]. The performance experiments were conducted with NaCl solutions of 10 and 35 g/L at feed pH of 7 ± 0.2 and temperature (25°C ± 1°C) to simulate brackish water and seawater, respectively. The determination of the total dissolved salt of the permeate water was measured by a pH/conductivity meter (430 portable, Jenway, England). The salt rejection was calculated by applying the following equation [14]:

$$\text{Rejection}\left(\%\right) = 100 \times \frac{\left(C_f - C_p\right)}{C_f} \quad (2)$$

where C_f and C_p are the ionic conductivity of feed solution and permeate, respectively.

The permeate water flux (L/m² h) is defined as:

$$\text{Flux} = \frac{V}{A \times t} \quad (3)$$

where V is the permeate volume (L), A is the membrane area (m²) and t is the time (h).

3. Results and discussion

3.1. Crystallinity of PA-TFC membranes

The XRD patterns of the DAT- and MPD-based PA membranes are shown in Fig. 1. The two XRD diffraction patterns of the DAT- and MPD-based PA membranes exhibited amorphous broad peaks at 2θ of 17.18° and 17.22°. The DAT- and MPD-based PA membranes that were prepared from aqueous phase containing TEA, IPA and CSA additives have d-spacing higher than the pristine membrane [12]. The d-spacing within the PA chains increases to 5.157 and 5.145 Å for DAT- and MPD-based PA membranes, respectively. This may be attributed to the interference of additives with the IP reaction [5,15].

3.2. PA membrane morphology

The characterization of the PA-TFC membranes skin surface layer, bottom and cross-section was done by the SEM micrographs. Fig. 2 depicts the SEM micrographs of pristine and PA membranes prepared at 6 wt% CSA, 3 wt% TEA, 4 wt% IPA and PS cast on polyester substrate. The SEM surface micrographs of the PA membranes prepared with and without additives shows dense and continuous skin layer with uniform ridge and valley topography similar to the pristine membrane. However, the surface image of PA membrane, which is prepared on polyester fabric, exhibits a less pronounced ridge and valley topography with many prominent cellular structures. The SEM bottom micrograph of the
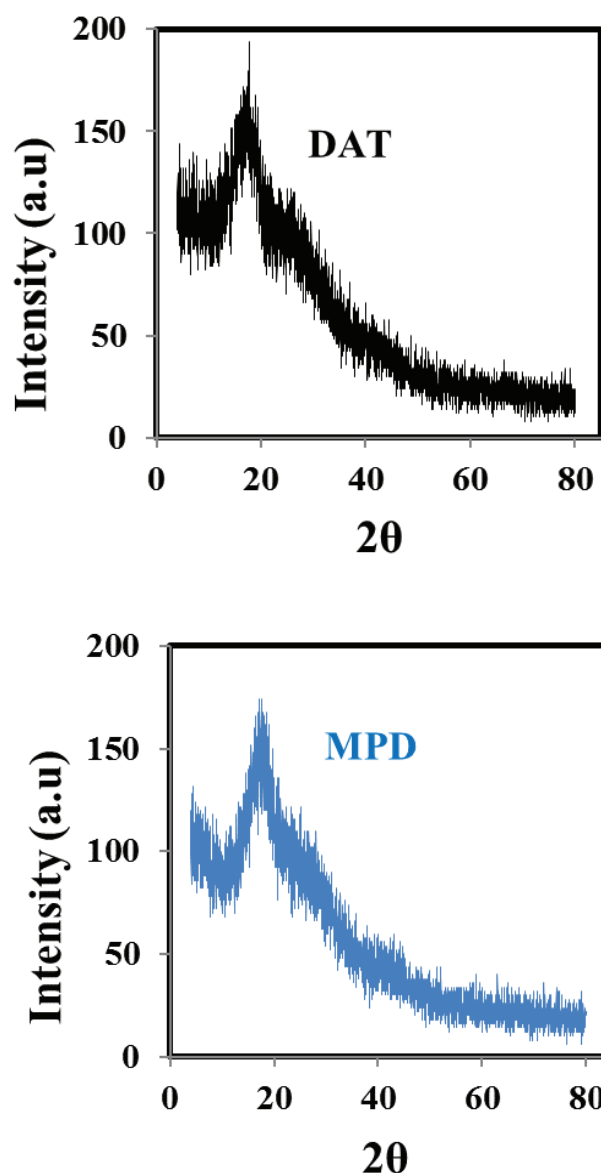
Fig. 1. XRD patterns of the DAT- and MPD-based PA membranes.

PA-TFC membranes, which are prepared with and without additives, shows a porous support membrane with different pore diameter. The bottom image of PA membrane casted on polyester fabric has a fiber-like structure related to the polyester fibers. From the SEM cross-sectional micrographs, the PA membrane layers are clearly distinguished. The dense skin PA forms the first layer with thickness of about 0.25 μm, the second PS support layer with about 67 μm and polyester third layer with about 45 μm. The PS support has thin passage channels with finger-like morphology.

3.3. Hydrophilicity of PA-TFC membranes

Fig. 3 represents the contact angle of the pristine and PA membranes prepared at different TEA concentrations and at different IPA concentrations. The contact angle has increased from 41.44° for pristine membrane to 49° at 1 wt% of TEA
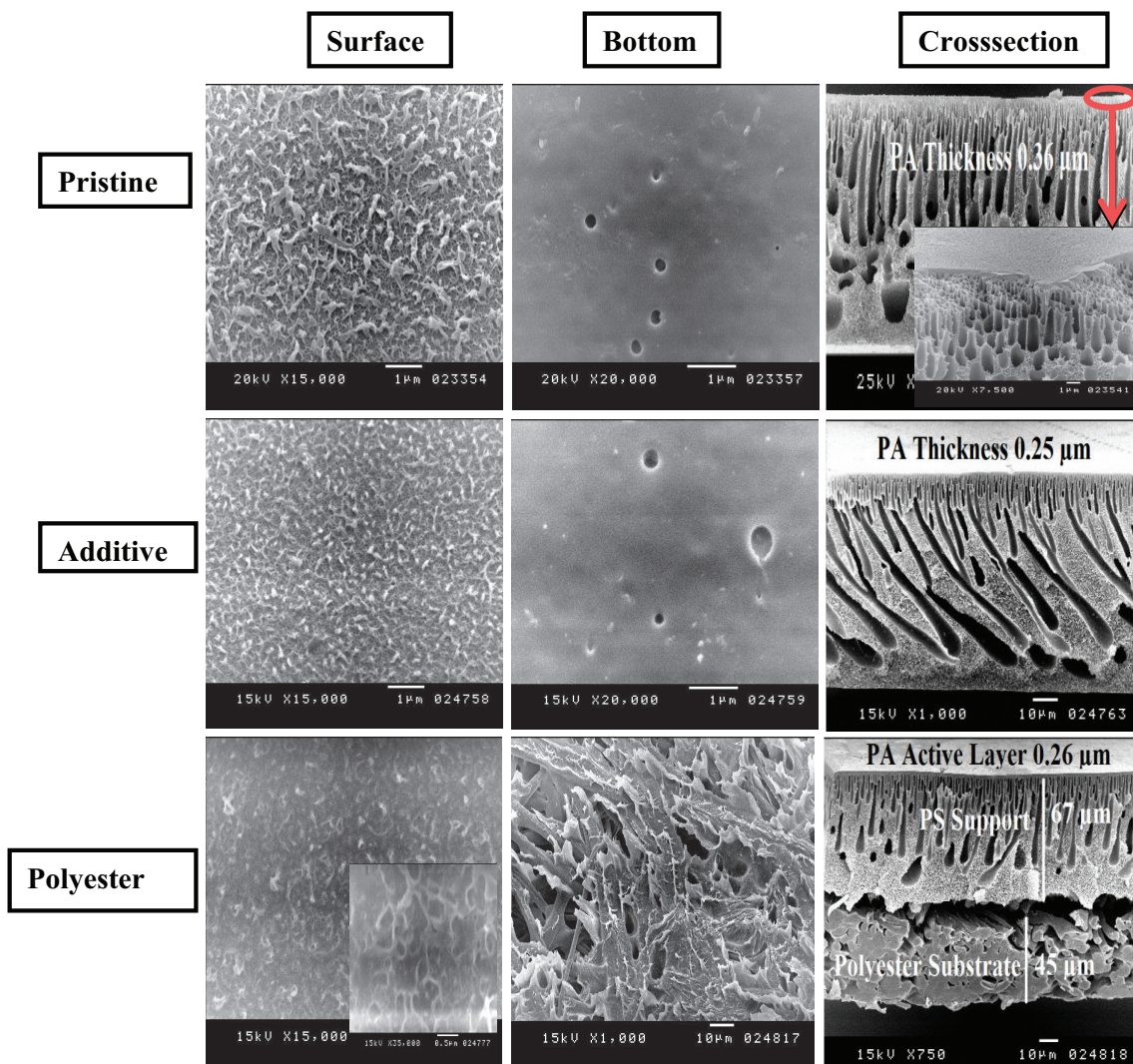
Fig. 2. SEM micrographs displaying the surface, bottom and cross-section of pristine and PA-TFC membranes prepared at 3 wt% TEA, 4 wt% IPA and 6 wt% CSA, and casted on polyester.

concentrations as shown in Fig. 3(A). The increase of TEA concentrations up to 3 wt% has decreased the contact angle value to 37.4°. This may be attributed to the initial decreases and subsequent gradual increases of the ionizable moieties in the PA network with incorporation of TEA [16–18]. The higher TEA concentration of 5 wt% caused a shift to higher contact angle of 48.8° due to the formation of thick and highly cross-linked PA film [5]. With increasing the IPA concentrations from 0 wt% (pristine membrane) to 4 wt%, the contact angle decreased from 41.44° to 35.44° due to the increases of the ionizable moieties in the PA network [16] as shown in Fig. 3(B). The contact angle has increased to 44.48° as the IPA concentration reached 8 wt%. The poor miscibility between IPA and hexane may probably have created a separation interface between ionizable moieties and the PA surface [19].

3.4. The PA membrane performance

The addition of TEA, IPA with CSA in the aqueous phase could increase the water flux, with no loss of salt rejection [15,17,20,21]. Therefore, the different additives concentration as well as casting the PS membrane over a polyester non-woven fabric as supporting substrate was studied to obtain an optimized set of conditions for the PA-TFC membrane performance enhancement. Adding the two additives together had a clearly positive effect on both the water flux and the stability [17,22]. The CSA additive was added to adjust the pH to around 9 and improve the absorption of the aqueous solution as well as to protect the microporous support membrane from pore coalescence or fusion during heat treatment [15,18,23].

3.4.1. Effect of TEA concentration on the PA membranes performance

The performance of the PA membranes that was prepared with different TEA concentration at different operating pressures in 10 g/L NaCl feed solution is presented in Fig. 4. The PA membranes were prepared at the optimum preparation condition and 2 wt% IPA, 6 wt% CSA as well as at different
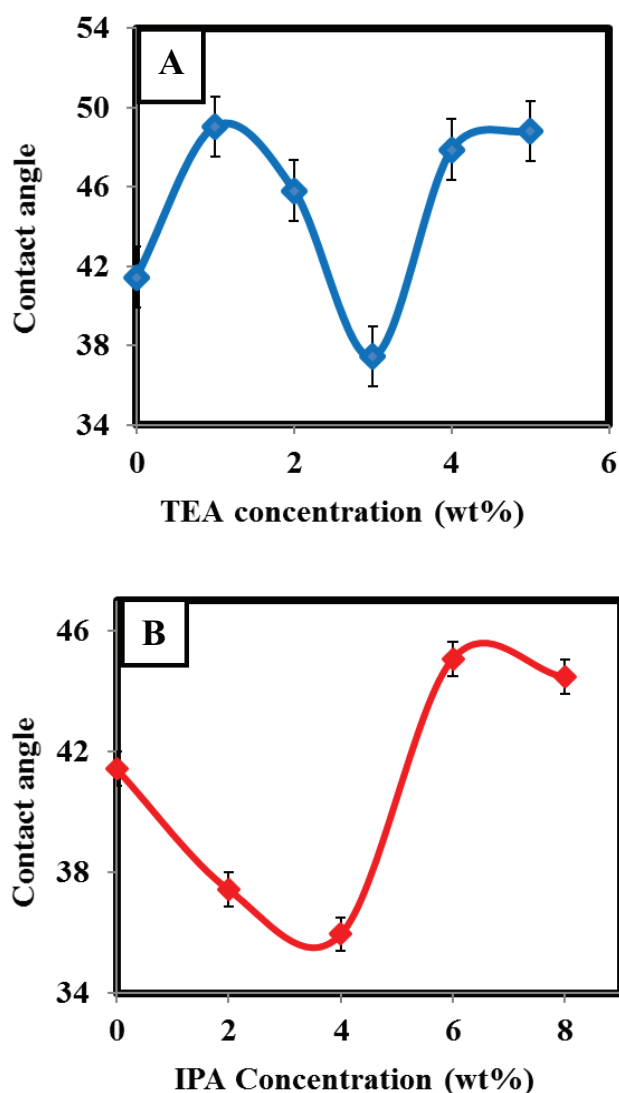
Fig. 3. Contact angle of PA membranes prepared at different TEA concentrations, 6 wt% CSA and 2 wt% IPA (A) and at different IPA concentrations, 6 wt% CSA and 3 wt% TEA (B).

Fig. 4. Salt rejection (A) and water flux (B) of the PA-TFC membranes prepared at different TEA concentrations using 10 g/L NaCl feed solution vs. operating pressure.

concentrations of TEA (1, 2, 3, 4 and 5 wt%). The experiments were conducted at 25°C and the pressure was varied from 16 to 26 bar to evaluate the membranes performance. It appeared from Fig. 4(A) that as the operating pressure increased from 16 to 26 bar, the salt rejection of the TFC membranes has increased until the pressure reached 18 bar and then the salt rejection decreased when reached 20 bar. The decline of the salt rejection at pressure exceeding 20 bar may be due to the breakdown of the active layer structure and/or concentration polarization [24]. The water flux of the membrane which was prepared at 3 wt% TEA, increased from 13.85 to 24.3 L/m² h with increasing the operating pressure from 16 to 26 bar as shown in Fig. 4(B).

The effects of the TEA concentrations on the desalination performance of the PA membranes (using 10 g/L NaCl feed solution at 18 bar) are plotted in Fig. 5. It is noted that the incorporation of TEA had a slight effect on the salt rejection while the water flux was remarkably improved. With the
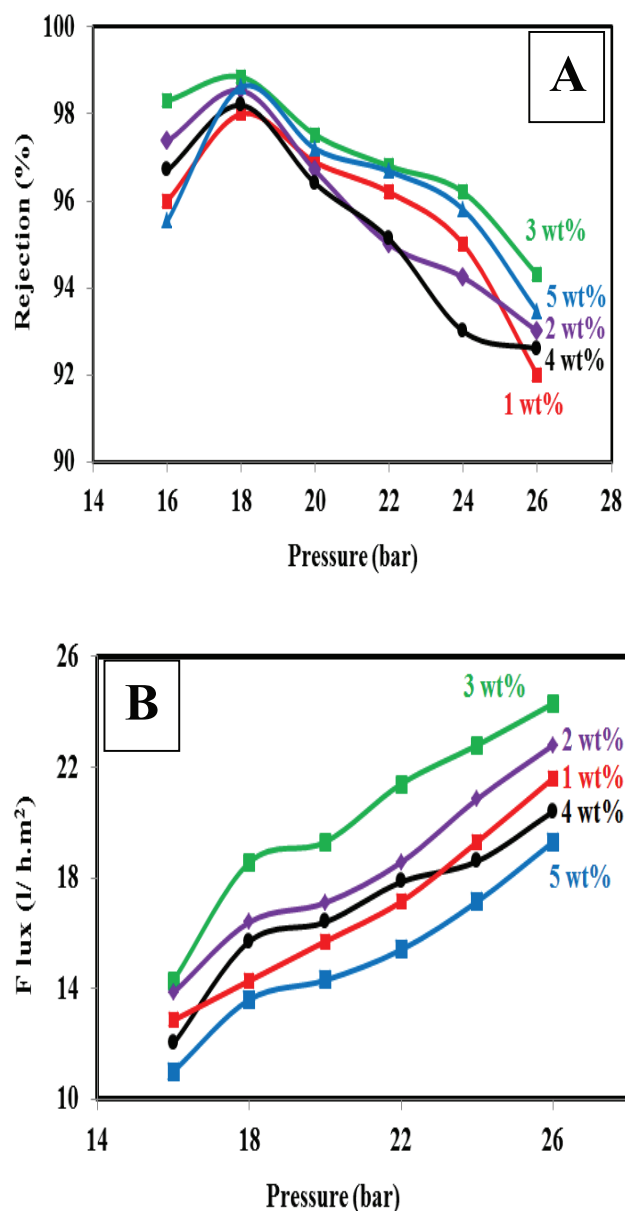
increase of TEA concentration from 1 to 5 wt%, the salt rejection is relatively stable. However, the water flux increased from 14.28 to 18.56 L/m² h with increasing TEA concentration from 1 to 3 wt% and then decreased again to 13.6 L/m² h at 5 wt%. The TEA not only acts as an acid acceptor but also acts as a catalyst for the acyl chloride and the amine reaction [5,17,18]. Therefore, the neutralization of the produced HCl and nucleophilic catalysis make the acylation of DAT by TMC faster in the presence of TEA than in its absence. The increases of the polymerization rate produce more thinner and cross-linked films, which explain the enhancement of water flux up to 3 wt% TEA without a loss of salt rejection [5]. However, at high concentrations of TEA than 3 wt%, the water flux has decreased due to the formation of high molecular weight PA
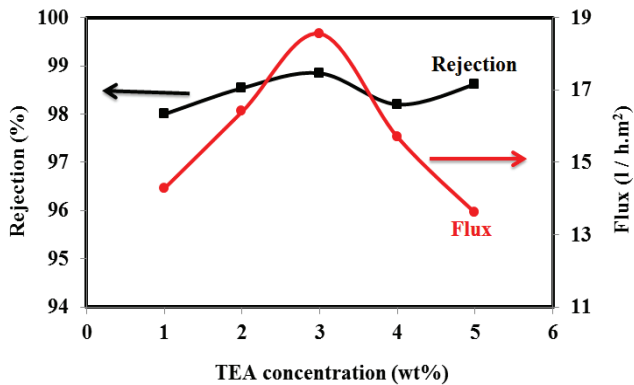
Fig. 5. Salt rejection and water flux of PA-TFC membranes vs. TEA concentrations using 10 g/L NaCl feed solution at 18 bar.

that results in a thick, dense skin layer on the membrane surface [25]. The membrane that was prepared at 3 wt% TEA exhibits the maximum salt rejection of 98.85% and water flux of 18.56 L/m^2 h at 18 bar. Also, the membrane capability to withstand high operating pressure without deformation was increased there by having a salt rejection of 94.3% at 26 bar.

3.4.2. Effect of IPA concentration on the PA membranes performance

Fig. 6 depicts the effect of the operating pressure on the salt rejection and water flux of the PA-TFC membranes prepared at different IPA concentrations in 10 g/L NaCl feed solution. The PA membranes were prepared at the optimum preparation condition and 6 wt% CSA and at 3 wt% TEA as well as different concentrations of IPA (2, 4, 6 and 8 wt%). With increasing the operating pressure from 16 to 26 bar, the salt rejection of the TFC membranes first increased and then the salt rejection decreased. However, the water flux has linearly increased over the measured range as depicted in Fig. 6(B). The water flux of the membrane prepared at 4 wt% IPA, increased from 17.1 to 27.85 L/m^2 h with increasing of the operating pressure from 16 to 26 bar.

The water flux and salt rejection of the PA membranes that was prepared with different concentrations of IPA in 10 wt% NaCl feed solution at 18 bar are plotted in Fig. 7. It was observed that the water flux has increased from 18.85 to 23.8 L/m^2 h while the salt rejection has slightly changed as the IPA concentration increased from 2 to 4 wt%. Addition of hydrophilic additives or alcohol to the amine solution enhanced the water flux of PA membranes with a good salt rejection of 98.85%. The incorporation of the IPA additive to the aqueous solution provides an additional pathway for the molecular transport of water and charge repulsion to maintain the salt rejection [15,26,27]. Also, the IPA facilitates the impregnation of the amine solution into the pores of the hydrophobic support membrane [18,28]. At higher IPA concentration of 8 wt% the water flux increased to 26.3 L/m^2 h while the salt rejection decreased to 96.2%. The decrease in the salt rejection can be attributed to the interference of IPA at higher concentration with the IP reaction forming deteriorated and loose skin PA layer which poorly rejects the salt while permeating more amounts of water
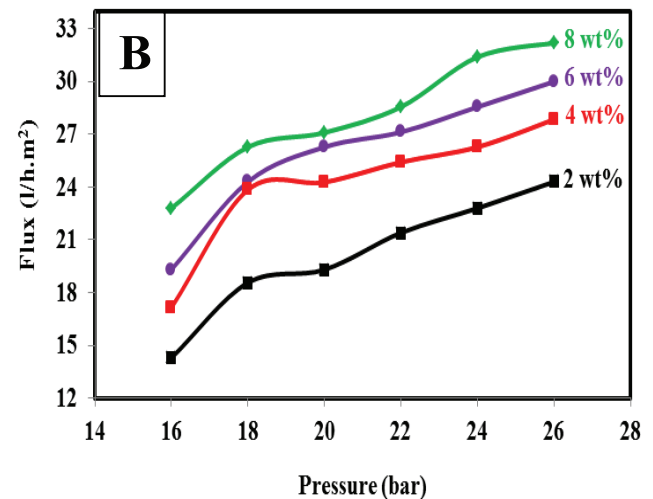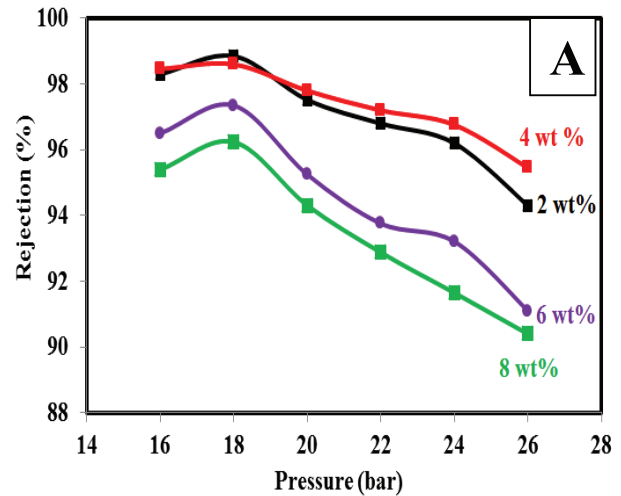
Fig. 6. Salt rejection (A) and water flux (B) of the PA-TFC membranes prepared at different IPA concentrations at 10 g/L NaCl feed solution vs. operating pressure.
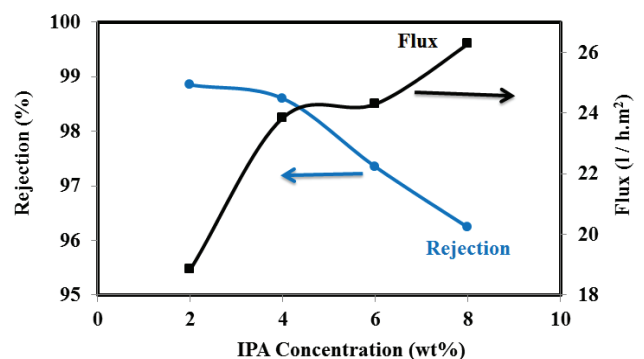
Fig. 7. Salt rejection and water flux of PA-TFC membranes and vs. IPA concentrations at 10 g/L NaCl feed solution at 18 bar.

[5,15]. The membrane that was prepared at 4 wt% optimum concentration of IPA exhibits the maximum salt rejection of 98.6% and water flux of 23.85 L/m^2 h at 18 bar. The membrane

capability to withstand high operating pressure without deformation was further increased there by having a salt rejection of 95.45% at 26 bar as shown in Fig. 6(A).

3.5. PA-TFC membranes casted on non-woven polyester fabric

For further improvement of the membrane stability, the PS membrane was casted over polyester as a supporting substrate. The PA membranes were prepared at the optimum preparation condition, 6 wt% CSA, 3 wt% TEA, 4 wt% IPA and casted over polyester non-woven fabric.

The salt rejection and water flux of the PA membranes casted onto non-woven polyester vs. the operating pressure at 10 wt% NaCl feed solution are shown in Fig. 8. As the operating pressure increases from 16 to 20 bar, the salt rejection of the PA membranes has slightly increased to 99.46% at 18 bar and then decreased to 98.4% at 20 bar. As the operating pressure increased to 26 bar, the membrane exhibited a salt rejection of 97.3% indicating a remarkable increase in the membrane capability to withstand high operating pressure without deformation. The use of the polyester as a substrate has increased the membrane mechanical properties and allowed for withstanding high pressure [29]. However, there is a linear relationship between the water flux and pressure over the entire pressure range. The water flux increases from 23.4 to 29.3 L/m^2 h with increasing the operating pressure from 16 to 26 bar. The optimum salt rejection of 99.46% and water flux of 25.3 L/m^2 h were achieved at 18 bar in 10 g/L NaCl feed solution and at 25°C. The energy consumed by the PA membrane which operated at these conditions is 0.45 kWh/m^3. It can be concluded that the optimization of additives concentration in aqueous solution and the casting of the PA membrane on a polyester non-woven fabric increase the water flux to 25.3 L/m^2 h and improves the desalination stability

3.6. Comparison of the PA membranes performance

The conventional monomer, MPD, is replaced by the DAT monomer in the PA membrane preparation and the performance was compared. The DAT- and MPD-based PA membranes were prepared at the optimum preparation condition and 6 wt% CSA, 3 wt% TEA, 4 wt% IPA as well as PS cast on polyester substrate.

3.6.1. Brackish water desalination

Salt rejection and water flux of MPD-based PA membrane casted onto non-woven polyester shows the same trend of the DAT-based membrane at different operating pressure in 10 g/L NaCl feed solution as depicted in Fig. 9. The water flux increased from 25.7 to 47.6 L/m^2 h with increasing the operating pressure from 30 to 65 bar. The maximum salt rejection of 97.85% and water flux of 38.6 L/m^2 h were obtained at 50 bar in 10 g/L NaCl feed solution. It is observed that the MPD-based membrane was operating at higher pressure (50 bar) than the DAT-based membrane (18 bar). This may be attributed to the increase of the interplanner distance within the DAT-based PA chains which was caused by the bulky methyl group as was confirmed by XRD study [30–32]. However, the water fluxes of MPD-based membrane were higher (38.6 L/m^2 h)
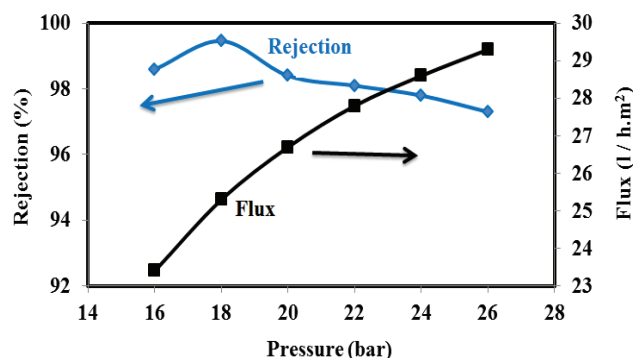
Fig. 8. Salt rejection and water flux of PA-TFC membrane cast onto non-woven polyester vs. operating pressure using 10 g/L NaCl feed solution.
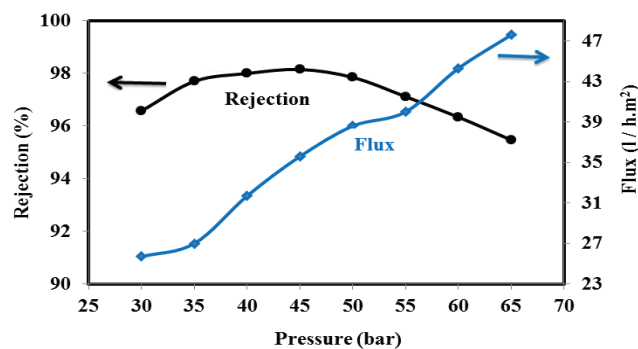
Fig. 9. Salt rejection and water flux of MPD-based PA membrane cast onto non-woven polyester vs. operating pressure in 10 g/L NaCl feed solution.

than the DAT-based (25.3 L/m^2 h) while the salt rejection was slightly changed at high pressure.

In a previous experiment, the commercial RO membrane (SW30-2540) exhibits a maximum salt rejection of 96.3% and water flux of 42.8 L/m^2 h in 10 g/L NaCl feed solution at 50 bar. The energy consumed by the MPD-based PA membrane and the commercial RO membrane is 0.78 and 0.73 kWh/m^3, respectively.

3.6.2. Seawater desalination

Fig. 10 shows the salt rejection and water flux of DAT- and MPD-based PA membranes vs. the operating pressure in 35 g/L NaCl feed solution. The performance of the two membranes showed the same trend. The DAT-based membrane showed a maximum salt rejection of 98.45% and water flux of 17.1 L/m^2 h at 35 bar. On the other hand, a maximum salt rejection of 96.85% and water flux of 25.1 L/m^2 h were observed at 55 bar for the MPD-based membrane. The DAT- and MPD-based membranes operating at these conditions have consumed energy of 1.129 and 1.42 kWh/m^3, respectively.

In a previous work [12], the optimum conditions for the preparation of MPD-based PA-TFC membrane were to soak 2 wt% of MPD for 2 min, 0.1 wt% of TMC for 1 min reaction time and curing at 70°C for 5 min. The membrane that was prepared at these conditions had a maximum salt rejection of 96% and water flux of 5 L/m^2 h in 10 g/L NaCl feed solution at
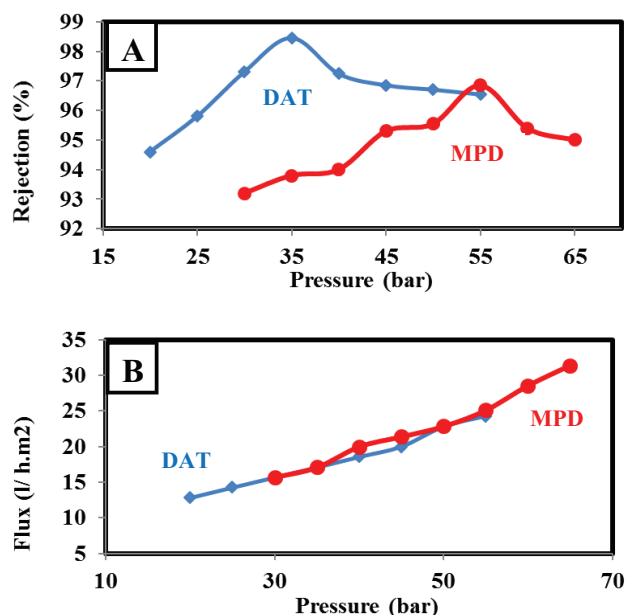
Fig. 10. Salt rejection (A) and water flux (B) of DAT- and MPD-based PA membranes vs. operating pressure in 35 g/L NaCl feed solution.

Fig. 11. The salt rejection (A) and water flux (B) of DAT- and MPD-based PA membranes through 3.5 h in 10 g/L NaCl feed solution at 18 and 50 bar.

55 bar. Also, the commercial membrane showed a salt rejection of 97% and water flux of 20 L/m² h in 35 g/L NaCl feed solution at 55 bar. The energy consumed by PA membrane which was prepared at optimum MPD condition and the commercial membrane is 3.57 and 1.55 kWh/m³, respectively. It was noted that the DAT-based membrane not only had reasonable salt rejection and water flux but also consumed lower energy than both the MPD-based and commercial membranes for brackish water and seawater desalination. Also, this membrane has lower energy consumption by 28.2% compared with the practical minimum energy consumption reported for RO system [33].

3.6.3. *Desalination performance stability*

The desalination performance stability of DAT- and MPD-based PA membranes measured through 3.5 h in 10 g/L NaCl feed solution at 18 and 50 bar, respectively, is shown in Fig. 11. The DAT-based membrane exhibited better long-term rejection stability but a lower water flux than the MPD-based membrane. Over the testing period, the salt rejection of the DAT-based membrane fluctuated between 99.37% and 96.68%, while the water flux fluctuated between 23.6 and 24.85 L/m² h. However, the salt rejection of the MPD-based membrane fluctuated between 98.2% and 92.82%, while the water flux of the DAT-based membrane fluctuated between 32 and 36 L/m² h.

4. Conclusions

The RO performance, especially the water flux and stability of PA-TFC membranes prepared by the IP reaction of DAT and TMC has been successfully enhanced by the incorporation of TEA, IPA and CSA additives in the aqueous phase solution as well as casting the PA membrane on non-woven polyester fabric. The optimal additives concentrations that gave the highest performance for the PA-TFC membrane were as follows: TEA = 3 wt%; IPA = 4 wt%; CSA = 6 wt% and PS casted on non-woven polyester fabric. The water flux of PA membrane which was prepared at these conditions was increased to 25.3 L/m² h, while the salt rejection reached 99.46% for a feed aqueous solution containing 10 g/L NaCl at 18 bar. For feed solution of 35 g/L NaCl, the prepared PA membrane exhibited a salt rejection of 98.45% and the water flux increased to 17.1 L/m² h at 35 bar. This membrane has good capability to withstand high operating pressure without compaction or deformation there by having a salt rejection of 97.3% at 26 bar. The DAT-based membrane not only had reasonable salt rejection and water flux but also consumed lower energy than both the MPD-based and the commercial membranes for brackish water and seawater desalination. The prepared membrane had lower energy consumption by 28.2% compared with the practical minimum energy consumption reported for RO system.

References

[1] H. Zou, Y. Jin, J. Yang, H. Dai, X. Yu, J. Xu, Synthesis and characterization of thin film composite reverse osmosis membranes via novel interfacial polymerization approach, Sep. Purif. Technol., 72 (2010) 256–262.

[2] W.J. Lau, A.F. Ismail, N. Misdan, M.A. Kassim, A recent progress in thin film composite membrane: a review, Desalination, 287 (2012) 190–199.

[3] B. Khorshidi, T. Thundat, B.A. Fleck, M. Sadrzadeh, Thin film composite polyamide membranes: parametric study on the influence of synthesis conditions, RSC Adv., 5 (2015) 54985–54997.

[4] W. Gao, F. She, J. Zhang, L. Dumée, L. He, P. Hodgson, L. Kong, Understanding water and ion transport behavior and permeability through poly (amide) thin film composite membrane, J. Membr. Sci., 487 (2015) 32–39.

[5] M. Liu, S. Yu, J. Tao, C. Gao, Preparation, structure characteristics and separation properties of thin-film composite polyamide-urethane seawater reverse osmosis membrane, J. Membr. Sci., 325 (2008) 947–956.

[6] R.J. Petersen, Composite reverse osmosis and nanofiltration membranes, J. Membr. Sci., 83 (1993) 81–150.

[7] S. Yua, M. Liu, X. Liu, C. Gao, Performance enhancement in interfacially synthesized thin-film composite polyamide-urethane reverse osmosis membrane for seawater desalination, J. Membr. Sci., 342 (2009) 313–320.

[8] X. Li, T. Chung, Effects of free volume in thin-film composite membranes on osmotic power generation, AIChE J., 59 (2013) 4749–4761.

[9] S. Zhang, F. Fu, T. Chung, Substrate modifications and alcohol treatment on thin film composite membranes for osmotic power, Chem. Eng. Sci., 87 (2013) 40–50.

[10] Y. Cui, X. Liu, T. Chung, Enhanced osmotic energy generation from salinity gradients by modifying thin film composite membranes, Chem. Eng. J., 242 (2014) 195–203.

[11] I. Kim, B. Jeong, S. Kim, K. Lee, Preparation of high flux thin film composite polyamide membrane: the effect of alkyl phosphate additives during interfacial polymerization, Desalination, 308 (2013) 111–114.

[12] M. Said, S. Ebrahim, A. Gad, S. Kandil, Toward energy efficient reverse osmosis polyamide thin film composite membrane based on diaminotoluene, Desal. Wat. Treat., 71 (2017) 261–270.

[13] M. Ding, A. Szymczyk, F. Goujon, A. Soldera, A. Ghoufi, Structure and dynamics of water confined in a polyamide reverse-osmosis membrane: a molecular-simulation study, J. Membr. Sci., 458 (2014) 236–244.

[14] S.H. Kim, S.Y. Kwak, T. Suzuki, positron annihilation spectroscopic evidence to demonstrate the flux enhancement mechanism in morphology controlled thin film composite (TFC) membrane, Environ. Sci. Technol., 39 (2005) 1764–1771.

[15] L. Zhao, P. Chang, W. Ho, High-flux reverse osmosis membranes incorporated with hydrophilic additives for brackish water desalination, Desalination, 308 (2013) 225–232.

[16] X.Z. Wang, L. Yu, J. Wang, S. Wang, A novel reverse osmosis membrane with regenerable anti-biofouling and chlorine resistant properties, J. Membr. Sci., 435 (2013) 80–91.

[17] S. Hermans, R. Bernstein, A. Volodin, I. Vankelecom, Study of synthesis parameters and active layer morphology of interfacially polymerized polyamide–polysulfone membranes, React. Funct. Polym., 86 (2015) 199–208.

[18] A. Ghosh, B. Jeong, X. Huang, E. Hoek, Impacts of reaction and curing conditions on polyamide composite reverse osmosis membrane properties, J. Membr. Sci., 311 (2008) 34–45.

[19] T. Kamada, T. Ohara, T. Shintani, T. Tsuru, Controlled surface morphology of polyamide membranes via the addition of co-solvent for improved permeate flux, J. Membr. Sci., 467 (2014) 303–312.

[20] M. Kuehne, R. Song, N. Li, R. Petersen, Flux enhancement in TFC RO membranes, Environ. Prog., 20 (2001) 23–25.

[21] C. Kong, M. Kanezashi, T. Yamomoto, T. Shintani, T. Tsuru, Controlled synthesis of high performance polyamide membrane with thin dense layer for water desalination, J. Membr. Sci., 362 (2010) 76.

[22] S. Hermans, H. Mariën, E. Dom, R. Bernstein, I. Vankelecom, Simplified synthesis route for interfacially polymerized polyamide membranes, J. Membr. Sci., 451 (2014) 148–156.

[23] D. Li, H. Wang, Recent developments in reverse osmosis desalination membranes, J. Mater. Chem., 20 (2010) 4551–4566.

[24] M. Liu, S. Yu, Q. Ming, Q. Pan, C. Gao, Impact of manufacture technique on seawater desalination performance of thin-film composite polyamide-urethane reverse osmosis membranes and their spiral wound elements, J. Membr. Sci., 348 (2010) 268–276.

[25] R.W. Baker, Membrane Technology and Application, Overview of Membrane Science and Technology, 2nd ed., John Wiley & Sons Ltd., England, 2004, pp. 1–6.

[26] N.Y. Yip, A. Tiraferri, W.A. Phillip, J.D. Schiffman, M. Elimelech, High performance thin film composite forward osmosis membrane, Environ. Sci. Technol., 44 (2010) 3812–3818.

[27] A. Ghosh, E. Hoek, Impacts of support membrane structure and chemistry on polyamide–polysulfone interfacial composite membranes, J. Membr. Sci., 336 (2009) 140–148.

[28] Y. Hussain, M. Al-Saleh, S. Ar-Ratrout, The effect of active layer non-uniformity on the flux and compaction of TFC membranes, Desalination, 328 (2013) 17–23.

[29] D. Enrico, G. Lidietta, Comprehensive Membrane Science and Engineering, Basic Aspects in Polymeric Membrane Preparation, 1st ed., Elsevier B.V., UK, 2010, pp. 91–93.

[30] J. Espeso, A. Lozano, J. de la Campa, J. de Abajo, Effect of substituents on the permeation properties of polyamide membranes, J. Membr. Sci., 280 (2006) 659–665.

[31] C. Nagel, K. Gunther-Schade, D. Fritsch, T. Strunskus, F. Faupel, Free volume and transport properties in highly selective polymer membranes, Macromolecules, 35 (2002) 2071–2077.

[32] K. Chang, Y. Huang, K. Lee, K. Tung, Free volume and polymeric structure analyses of aromatic polyamide membranes: a molecular simulation and experimental study, J. Membr. Sci., 354 (2010) 93–100.

[33] M. Ding, A. Ghoufi, A. Szymczyk, Molecular simulations of polyamide reverse osmosis membranes, Desalination, 343 (2014) 48–53.